Heliyon 10 (2024) e39402

Contents lists available at ScienceDirect

Heliyon

journal homepage: www.cell.com/heliyon

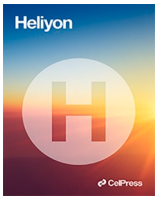

Research article

Downregulation of aquaporins and PI3K/AKT and upregulation of PTEN expression induced by the flavone scutellarein in human colon cancer cell lines

Noor Tarawneh [a], Lama Hamadneh [a,b], Walhan Alshaer [c], Abdel Qader Al Bawab [a], Yasser Bustanji [d,e], Shtaywy Abdalla [f,*]

[a] Department of Pharmacy, Faculty of Pharmacy, Al-Zaytoonah University, Amman, 11733, Jordan
[b] Department of Basic Medical Sciences, Al-Balqa Applied University, Al-Salt, 19117, Jordan
[c] Cell Therapy Center, The University of Jordan, Jordan
[d] Department of Basic Medical Sciences, College of Medicine, University of Sharjah, Sharjah, United Arab Emirates
[e] Department of Department of Biopharmaceutics and Clinical Pharmacy, School of Pharmacy, The University of Jordan, Amman, 11942, Jordan
[f] Department of Biological Sciences, School of Science, The University of Jordan, Amman, 11942, Jordan

ARTICLE INFO

Keywords:
Aquaporins
Apoptosis
Colorectal cancer
Metastasis
PI3K/AKT signaling
PTEN
Scutellarein

ABSTRACT

Scutellarein has an anticancer potential, but the pathway of its action has not been elucidated. This study investigated scutellarein efficacy against human colorectal cancer (CRC) and explored the possible pathway of its action. MTT assay was employed to detect scutellarein effect on HT-29, SW-480, and HCT116 cells viability. Scutellarein impact on programmed cell death was studied by Annexin V-FITC/PI and its role on migration and invasion was detected by wound healing and transwell chambers. Aquaporin (AQP) 1, 3, and 5 expression before and after scutellarein treatment was approached by quantitative polymerase chain reaction (RT−qPCR) and immunostaining while Western blotting was used to explore scutellarein effect on PI3K/AKT pathway. Scutellarein induced apoptosis and necrosis in CRC cells, thus inhibiting proliferation, migration, and invasion. Colon cancer cells exhibited positive staining for AQP 1, 3, and 5 which was downregulated by scutellarein. PI3K/AKT pathway mediating cell proliferation and growth was also modulated by scutellarein; phosphatase and tensin (PTEN) was upregulated, whereas PI3K, AKT, and p-AKT expressions were downregulated, and the downstream mTOR and phosphorylated mTOR were also suppressed at the protein level. Data indicated that scutellarein suppressed growth, migration as well as invasion of these CRC cells by downregulating the expression of *AQP 1*, *3*, and *5* and upregulating *PTEN* where the latter inhibited the genes and the proteins involved in *PI3K/AKT* pathway. The data indicate that scutellarein is a promising therapeutic agent that inhibits growth, migration, and invasion of CRC cells by down-regulating the expression of AQP 1, 3, and 5 and by PTEN up-regulation, thus inhibiting PI3K/AKT. These molecular alterations represent potential prognostic biomarkers for the metastasis of colon cancer, where the down-regulation of AQPs enhances patient survival.

* Corresponding author.
E-mail addresses: n.tarawneh@zuj.edu.jo (N. Tarawneh), lama.hamadneh@bau.edu.jo (L. Hamadneh), walhan.alshaer@ju.edu.jo (W. Alshaer), bustanji@ju.edu.jo (Y. Bustanji), shtaywy@ju.edu.jo (S. Abdalla).

https://doi.org/10.1016/j.heliyon.2024.e39402
Received 8 June 2024; Received in revised form 14 October 2024; Accepted 14 October 2024
Available online 15 October 2024

1. Introduction

Colon cancer is a malignant tumor, and its incidence is increasing, where the number of deaths are expected to increase by 71.5 % in the coming two decades [1]. The current management of cancer patients is accompanied by deleterious side effects, a matter that prompts an increasing demand for additional therapeutic options for cancer management. These new therapies should optimally have low toxicity, high efficacy in inhibiting cancer cells proliferation but, more importantly, in controlling invasion and metastasis. Metastasis is a limiting factor for treatment success and for cancer patients' recovery in many cancer patients [2]. Invasion and metastasis, which both depend on cell motility, have been correlated positively with the water channel proteins aquaporins (AQPs) expression [3,4].

AQPs exhibit diverse physiological roles and are abundant in a wide range of tissues within the human body. AQPs 1, 2, 3, 4, 5, 8, and 9 have been implicated in the processes of cancer invasion and metastasis [5], since they regulate adhesion of cell-to-cell, cell-to-matrix, epithelial-mesenchymal transition, protease and extracellular-matrix degrading molecule, interaction with the actin cytoskeleton, and interaction with pathways that enable motility and invasion, thus promoting cancer progression [6]. Pharmacological modulators of aquaporin channels have been tested for therapeutic efficacy, including compounds that serve as loop diuretics [7], and some metallo-organic compounds [8].

Current cancer chemotherapies have varying levels of effectiveness, but they lack specificity and have significant side effects [9]. Natural products have received significant attention in research, offering a promising opportunity for the identification of new anti-cancer compounds [10,11]. Scutellarein (4′,5,6,7-tetrahydroxyflavone), a compound found in dried herbs used in Chinese folk medicine, has shown significant antineoplastic effects, besides other effects [12,13]. It demonstrated antitumor effects on colorectal cancer, indicating its potential as a promising therapeutic agent for antitumor interventions [13,14].

Scutellarein was proposed to decrease cell viability and increase apoptosis by different mechanisms. Chang et al. (2014) showed that scutellarein inhibited lung cancer cells proliferation through nuclear factor-κB (NF-κB) and through signaling by mitogen-activated protein kinase (MAPK) [15]. Shi et al. [16]. showed that scutellarein can increase reactive oxygen species (ROS) production and lead to membrane potential collapse in mitochondria of HCT116 cells. Likewise, Guo et al. [17] showed that scutellarein caused human colon cancer HCT116 cells apoptosis by a pathway that is ROS-mediated in the mitochondria, since it downregulated Bcl-2 and upregulated Bax. Moreover, Li et al. [18] showed that scutellarein inhibitory effect occurs through upregulation of CDC4-mediated ubiquitination of advanced glycation end products (RAGE) receptor in colon cancer T84 and SW-480 cells, whereas Lang et al. [19] proposed that the inhibitory effect of scutellarein occurs through its downregulation of enhancer of zeste homolog 2 (EZH2), a histone methyltransferase that is closely correlated in several human malignancies with tumor aggressiveness, and the upregulation of forkhead box protein O1 (FOXO1) expression, which negatively regulates PI3K/AKT. The complex nature of scutellarein effects has led us to explore its potential in inhibiting the spread of colon tumors. The literature indicates that aquaporins (AQPs) impact colorectal cancer (CRC) cells migration and metastasis [4,20]. This suggests that AQPs could be important targets for prognosis and therapy in colon tumor metastasis as has been suggested by others' work [21,22].

This work examined the expression levels of AQP1, AQP3, and AQP5 in HT-29, SW-480, and HCT-116 CRC cells. The objective was testing the hypothesis that AQPs are down-regulated by scutellarein and if this down-regulation was concomitant with suppression of migration and metastasis in these cell types. Furthermore, we also examined whether scutellarein affects the expression of components within the PI3K/AKT pathway. This pathway plays a crucial role in mediating growth factors actions that facilitate tumor growth and development. Specifically, we examined scutellarein impact on phosphatase and tensin (PTEN), a tumor suppressor molecule, as well as the downstream components regulated by PTEN, including PI3K, AKT, and the downstream target mTOR.

2. Materials and methods

2.1. Cell culture

We employed the following three human colorectal cancer cell lines, HT-29, SW-480, and HCT-116 (Sigma Aldrich). The cells were grown in Dulbecco's modified Eagle's medium (DMEM) with a high glucose concentration of 4.5 g/L and supplemented with 10 % fetal bovine serum (FBS) and 1 % mixture of penicillin and streptomycin. The cells were cultured in 25-cm^2 T-flasks (Corning, New York, USA) and maintained in an incubator at standard conditions of 37 °C and a CO_2 level of 5 % [23].

2.2. Cytotoxicity of scutellarein

Viability of cells was evaluated by the MTT test. Cells were seeded in 96-well plates (density of 1×10^4 cells/well) then incubated under the conditions specified above. Normal fibroblasts were also seeded in some wells to check for the cytotoxicity of scutellarein for normal cells and were treated similar to the cancer cell lines. The cells were incubated with scutellarein (Biopurify Phytochemicals Ltd., Chengdu, China; Cat BP 1277) at doses ranging from 3 to 300 μM. Scutellarein was dissolved in dimethyl sulfoxide (DMSO). Following a 72-h incubation period, the media was substituted with RPMI-1640 media supplemented with FBS (5 %). 15 μL of MTT reagent (5 mg MTT/mL of PBS) were added to each well and incubated for 3 h at 37 °C. Subsequently, the medium was meticulously removed, and the formazan crystals present within cells were dissolved using a 100 μL solubilization/stop mix over a duration of 24 h. Following a 1-min period of agitation, absorbance was measured using a microplate reader (BioTek elx808, Agilent Technologies, Inc., USA) at 570 nm wavelength [23,24]. The impact of scutellarein on growth was assessed by determining the percentage of viability, which was calculated according to:

$$\text{Viability \%} = \frac{[\text{Mean optical density of the sample}]}{[\text{Mean optical density of the control}]} \times 100$$

IC_{50} values for cell lines were determined by performing three independent measurements using the 8th version of GraphPad Prism software.

2.3. Toluidine blue assay

Toluidine blue was used to evaluate the presence and quantity of substances, like nucleic acids and proteins. Cell counting was performed using trypan blue (Sigma-Aldrich, Budapest, Hungary) and a hemocytometer. A population of cells, consisting of 2×10^5 cells, was cultivated in 6-well plates and permitted to proliferate until a confluence level of 80–85 %. The cells were incubated at 37 °C for 72 h with scutellarein at predefined IC_{50} concentrations for each cell type (30.2, 99.2, and 76.9 μM, respectively). The previous media was extracted, and the cells underwent two washes with PBS (1 mL/well) for 5 min each. Subsequently, a solution of 1 % toluidine blue (Sigma-Aldrich) was applied [25]. The cellular morphology was analyzed, and visual documentation was achieved by ZEISS Axio Vert.A1 microscope outfitted with a Leica Flexacam1 camera.

2.4. Flow cytometry

Cell lines were cultivated at a seeding density of 1×10^6 cells per flask at the following conditions: 37 °C, 5 % CO_2, 95 % relative humidity until a 80–85 % confluence. The cells were incubated with scutellarein (3, 10, 30, 100, and 300 μM) for 24, 48, or 72 h. The control cells for this experiment and the following experiments were colorectal cells of the same type as that of the cell line studied and they were treated with the solvent of scutellarein (i.e., DMSO) using the same volume as that of the treatments. The cells were then stained as per the instructions of the manufacturer (Promega, Minneapolis, MN 55413, USA). Briefly, the cells were dislodged and gathered along with their respective media, subjected to a cold PBS wash and centrifuged at 1500 rpm for a duration of 10 min at ambient temperature. The solid particles were reconstituted in 500 μL of cold binding buffer (1X) and subjected to centrifugation once more. The cells were resuspended in Annexin V reagent that is composed of 10 μL of binding buffer (10X), 10 μL of propidium iodide, 1 μL of Annexin V-FITC, and 79 μL of distilled H_2O, resulting in a total volume of 100 μL in each tube. Following a 15-min incubation period, 400 μL of ice-cold binding buffer (1X) was added, subsequently fluorescence analysis was conducted within 1 h of the staining process. Quantification was performed with a BD Accuri™ C6 Plus Flow Cytometer, (BD Medical Devices Co., USA). A total of 10,000 to 20,000 events were gathered for each sample. The outcomes were presented in dot plots categorized into four quadrants: (AN-/PI-) to represent viable cells, (AN+/PI-) to represent early apoptosis, (AN+/PI+) to represent late apoptosis, and (AN-/PI+) to represent necrosis. The excitation wavelength was 488 nm. The fluorescence emitted by Annexin V-FITC was identified in the FL1 channel, utilizing a bandpass filter with an emission range of 533/30 and, propidium iodide fluorescence was detected in the FL2 channel, utilizing a bandpass filter with an emission range of 585/40. The experimental conditions employed in this study involved the utilization of double-stained cells that were left untreated [26].

2.5. Wound healing assay

To assess cellular migration, cell lines were seeded in 6-well plates with seeding density of 1.6×10^5 cells/well. Cells were then allowed to a confluence of 85–90 % at 37 °C and 5 % CO_2 in 24 h. Monolayers were mechanically disrupted by creating scratches with a 200 μL-pipette tip. Subsequently, media were removed, and cells were meticulously rinsed with PBS in order to eliminate any cells or debris that were freely suspended. Cells were incubated in FBS-free DMEM, treated with scutellarein (3, 10, 30, 100, and 300 μM), and cells movement towards wound site was documented and quantified with a ZEISS Axio Vert. A1 microscope outfitted with a Leica Flexacam1 camera, at a magnification of 10X (Boeco, Hamburg, Germany). Width of wound was measured at 0, 24, 48, and 72 h. The quantification of wound closure was determined by calculating percent reduction in the normalized area over the initial open area according to:

$$\text{Wound Closure \%} = \frac{A(0) - A(t)}{A(0)} \times 100,$$

where $A(0)$ is the area at time zero (0) and $A(t)$ is the area after incubation time (t) [27].

2.6. Migration assay

The migratory characteristics of a cell line was assessed by transwell chambers equipped with filters of pore size of 8.0 μm (Corning Inc., Cambridge, MA, USA). A population of cells (1×10^5) was introduced into the upper chamber, and incubated at 37 °C to a confluence of 85–90 %. Media in the upper chamber was aspirated, substituted by serum-free media for a duration of 24 h and a medium consisting of 10 % FBS was introduced into the lower chamber as a positive control and a chemoattractant. The cells were incubated to migrate for 72 h, in the absence or the presence of scutellarein (IC_{50} specific to each cell line). Migrating cells were fixed using a 4 % paraformaldehyde for 10 min, followed by permeabilization in 100 % methanol for 2 min. The cells present in the transwell chamber filter were stained with 2 % crystal violet (C3886, Sigma). Images of migratory cells from five randomly chosen fields were captured, enumerated, and their count was reported as a percentage relative to the control group [28].

2.7. Invasion assay

Invasion capacity of cells was evaluated by Matrigel precoated transwell chambers equipped with filters that have a pore size of 8.0 μm (Corning Inc., Cambridge, MA, USA). 30–40 μL of Matrigel was introduced into a 12-well transwell insert and allowed to solidify at 37 °C within an incubator for 15–30 min to give a thin layer of gel. 1×10^5 cells were seeded into the upper chamber, incubated at 37 °C to a confluence of 85–90 %, and the medium in the upper chamber was then aspirated, substituted with serum-free media and the cells were incubated for 24 h. In the lower chamber, a medium consisting of 10 % FBS was employed as a chemoattractant and to serve as a positive control. The cells were incubated to migrate for 72 h in the absence or the presence of scutellarein as described in the migration assay. The cells that successfully traversed the Matrigel were subsequently processed as described above. The number of cells in each field was then tallied and expressed as a percentage relative to the control group [29].

2.8. Staining protocol for aquaporins (immunofluorescence)

Cells were seeded at a density of 1×10^4 cells/well in 6-well plates with sterile coverslips and were cultured for 24 h, incubated for 72 h with scutellarein at its IC_{50} concentration, and the cells that adhered to the coverslips were rinsed twice with PBS, fixed at ambient temperature for 10 min. Following three washes with PBS for 5 min, the cells underwent permeabilization using PBS supplemented with 0.3 % Triton-X100 for 5 min. Subsequently, the cells were blocked using 5 % normal goat serum (NGS) for 30 min. Immunofluorescence labeling was done by overnight incubation of the coverslips with the cells attached to them at 4 °C with primary antibodies targeting aquaporin proteins (AQP1, AQP3, and AQP5) at a dilution ratio of 1:50. The cells then underwent four washes in PBS for 5 min each. Subsequently, they were subjected to another blocking step using PBS containing 5 % NGS. The cells were then incubated in the presence of a goat anti-rabbit IgG (H + L) secondary antibody labeled with fluorescein isothiocyanate (FITC) at a dilution of 1:200. The incubation was carried out in the dark for 1 h. The specific antibody used in this experiment was VK307556 (Invitrogen, USA). The cell lines underwent two washes in PBS for 5 min each, then incubated for 5 min with DAPI (300 nM) for nuclear staining. The cells underwent two further washes with PBS, placed onto glass slides, images were captured using an Olympus CKX41 inverted phase contrast fluorescence microscope fitted with an Optika Pro5 camera (Microscope Central, Tustin, CA, USA). The density of fluorescence was quantified, and the determination of the mean adjusted total cell fluorescence was performed using ImageJ V1.8.0 software (software 1.48q, Rayne Rasband, National Institutes of Health, USA; http://rsb.info.nih.gov/ij/(NIH)) [30].

2.9. Reverse transcription-quantitative PCR (RT–qPCR)

Cell lines were seeded in T25 culture flasks at a density of 1×10^6 cells per flask at 37 °C, 5 % CO_2, and 95 % relative humidity to reach 80–85 % confluence. The cells were incubated with scutellarein (3, 10, 30, 100, or 300 μM) for 24, 48, or 72 h [31]. Total RNA extraction was performed using a commercially available SV Total RNA Isolation System kit (Promega, Minneapolis, MN 55413, USA) [32]. Initial cDNA strand was generated via the GoScriptTM Reverse Transcriptase System (Promega, USA) [33]. The cDNA synthesis process utilized a Bio-Rad PTC-200 temperature Cycler PCR 96-well instrument (Bio-Rad, Hercules, CA, USA). The temperatures employed for cDNA synthesis were as follows: A temperature of 95 °C for 2 min, followed by a series of 40 cycles. Each cycle involved subjecting the samples to 95 °C for 5 s, then 60 °C for 30 s. Subsequently, the microcentrifuge tubes were subjected to incubation at 4 °C for 24 h. The forward and reverse primer pairs for the intended genes (PTEN, PI3K, AQP1, AQP3, and AQP5) and the housekeeping gene (GAPDH) were obtained from Integrated DNA Technologies (IDT), USA. The primers were selected according to the methodology outlined in the relevant literature (Table 1). The expression levels of mRNA for target genes were evaluated by employing the Sso Advanced Universal SYBR® Green Supermix (Bio-Rad, USA). The PCR amplification was conducted using an RT-qPCR CFX96 real-time PCR system (Bio-Rad, USA), following the specified cycling conditions. The calculation of fold change was performed via the $2^{-\Delta\Delta Ct}$ methodology.

Table 1
Primers sequences employed for amplification of PTEN, PI3K, AQP1, AQP3, AQP5 and GAPDH genes.

Target gene	Primer sequence	Reference
PTEN	Forward: 5' CAAGATGATGTTTGAAACTAT 3' Reverse: 5' CTTTAGCTGGCAGACCACAA 3'	[34]
PI3K	Forward: 5' GAAGTTGCTCTACCCAGTGTCC 3' Reverse: 5' GATAGCCGTTCTTTCATTTGG 3'	[35]
AQP1	Forward: 5' ATT TTCTGG GTG GGGCCATT 3' Reverse: 5' GGG CCAGACCCCTTC TAT TT 3'	[36]
AQP3	Forward: 5' ACC CCT CTG GAC ACT TGG AT 3' Reverse: 5' GGGTTG TTGTAG GGGTCAA 3'	[36]
AQP5	Forward: 5' TCC ATTGGCCTGTCTGTCAC 3' Reverse: 5' CTT TGATGATGGCCACACGC 3'	[37]
GAPDH	Forward: 5' CATCACTGC CACCCAGAA GA 3' Reverse: 5' GTCAAAGGTGGAGGAGTGGG 3'	[37]

2.10. Western blot analyses

Impact of scutellarein on the PTEN/AKT/mTOR pathway in the three cell lines was examined using Western blotting according to Ref. [38]. Cell lines were cultured into T25 culture flasks with a density of 1×10^6 cells per flask to 85–90 % confluence. The cells were then incubated with scutellarein (0, 10, 30, and 100 μM) for 72 h at the standard conditions. The extraction of total protein from cells was performed using a RIPA lysis buffer, to which a phosphatase inhibitor cocktail IV (ab201115; Abcam, Cambridge, UK) was added. The bicinchoninic acid (BCA) protein assay kit was utilized to determine the total protein. Each lane of the gel contained 20 μg of target protein, which were separated using 8 % SDS-PAGE and subsequently transferred onto PVDF membranes. These membranes were then blocked for overnight at room temperature using 3 % BSA in Tris-buffered saline (TBS). The membranes were then incubated for overnight at 4 °C with the primary antibodies listed below: The antibodies used were PTEN (AF847, R&D System; dilution 1:1000), AKT (MAB2055, R&D System; dilution 1:1000), p-AKT-S473 (AF887, R&D System; dilution 1:1000), mTOR (AHO1232, Thermo Fisher Scientific; dilution 1:1000), p-mTOR-S2448 (ab109268, Abcam; dilution 1:1000), and beta actin (GW0061R; GenoChem World, S. L.; Valencia, del Parc, Spain; dilution 1:1000). The membranes were then washed using TBS and Tween®20 and incubated for 1 h at room temperature with a secondary antibody, specifically HRP-conjugated goat anti-rabbit antibody (AS014, ABclonal), at a dilution of 1:1000. The visualization of protein bands was achieved by employing the SuperSignal™ West Pico PLUS chemiluminescent substrate on a gel imaging system (GE Healthcare, Buckinghamshire, UK). Subsequently, the densitometric analysis of the band density was conducted using ImageJ V1.8.0 software.

2.11. Statistical analyses

Statistical analysis and image representations of data were performed using 8th version of Graph Pad Prism. Data are expressed as the means ±the standard deviation (SD). The wound healing trials were evaluated by statistical analysis using a one-way analysis of variance (ANOVA) followed by Dunnett's multiple comparisons test. Migration and invasion were analyzed using a two-way analysis of variance followed by Sidak's multiple comparisons test. The immunofluorescence investigations were conducted utilizing a paired *t*-test. The analysis of gene expression and Western blot studies were conducted using a two-way analysis of variance followed by Dunnett's multiple comparisons test. Statistical significance was considered when $p < 0.05$.

3. Results

3.1. Cytotoxicity of scutellarein

Fig. 1 indicates that scutellarein (30, 100, and 300 μM) demonstrated inhibitory effects on HT-29, SW-480, and HCT-116 cells viability. The inhibitory effects observed in smaller doses (3 and 10 μM) were relatively weak. The IC_{50} values were determined to be 30.2 ± 0.43, 99.2 ± 0.33, and 76.9 ± 0.27 μM for these cell lines, respectively. Normal fibroblast cells were not inhibited by the lowest dose of scutellarein and only modestly inhibited by 100 and 300 μM.

3.2. Toluidine blue assay

The influence of scutellarein (IC_{50} = 30.2 μM) on the HT-29 colon cell line revealed significant morphological changes. Morphological criteria of apoptosis in HT-29 cells, such as chromatin condensation, cell swelling, nuclear fragmentation, apoptotic

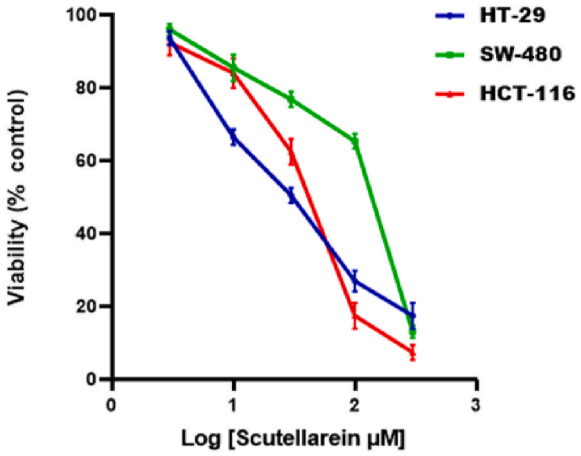

Fig. 1. Scutellarein inhibitory effects on the viability of the indicated cell lines. After 72 h of incubation with the specified concentrations of scutellarein, viability was assessed using the MTT assay. Data were evaluated using one-way ANOVA (F = 27.9541; P = 0.1313) and represent the means and standard deviations of three separate tests. The percentage of viability in comparison to untreated cells is used to express the values.

bodies (Fig. 2A), and vacuolated cytoplasm (Fig. 2B), were observed after 72 h. Similarly, an apoptotic effect of scutellarein on SW-480 cells (IC_{50} = 99.2 μM) was represented by swollen cells with fragmented nuclei and plasma membrane blebbing (Fig. 2C), as well as ruptured plasma membranes and vacuolated cytoplasm (Fig. 2D). In the HCT-116 cell line, scutellarein (IC_{50} = 76.9 μM) caused apoptotic features, including a fragmented nucleus, vacuolated cytoplasm, apoptotic bodies (Fig. 2E), chromatin condensation, a ruptured plasma membrane, and plasma membrane blebbing (Fig. 2F).

3.3. Flow cytometry

Fig. 3 shows that when HT-29 cells were treated with scutellarein (3, 10, 30, 100, and 300 μM), flow cytometry analysis revealed a gradual increase in apoptosis from 0.4 % to 13.4 % after 24 h, 32.9 % after 48 h, and 43.3 % after 72 h at 300 μM of scutellarein, while necrosis increased from 0.2 % to 22.8 % after 24 h, 11.8 % after 48hrs., and 9.5 % after 72 h. A similar trend of scutellarein impact was observed when SW-480 and HCT-116 cells were preincubated with scutellarein. Apoptosis values for SW-480 cells at 300 μM were 26.3 %, 31.1 %, and 33.8 % after 24, 48, and 72 h, respectively. Apoptosis values for HCT-116 cells were 6.3 %, 2.7 %, and 36.8 % for the same incubation periods at 300 μM. A graphical summary of the apoptotic and necrotic values for these cell lines is shown in Fig. 3 A, B, and **C** and complete display of the flow cytometry plots is appended as supplementary material (Fig. S1)

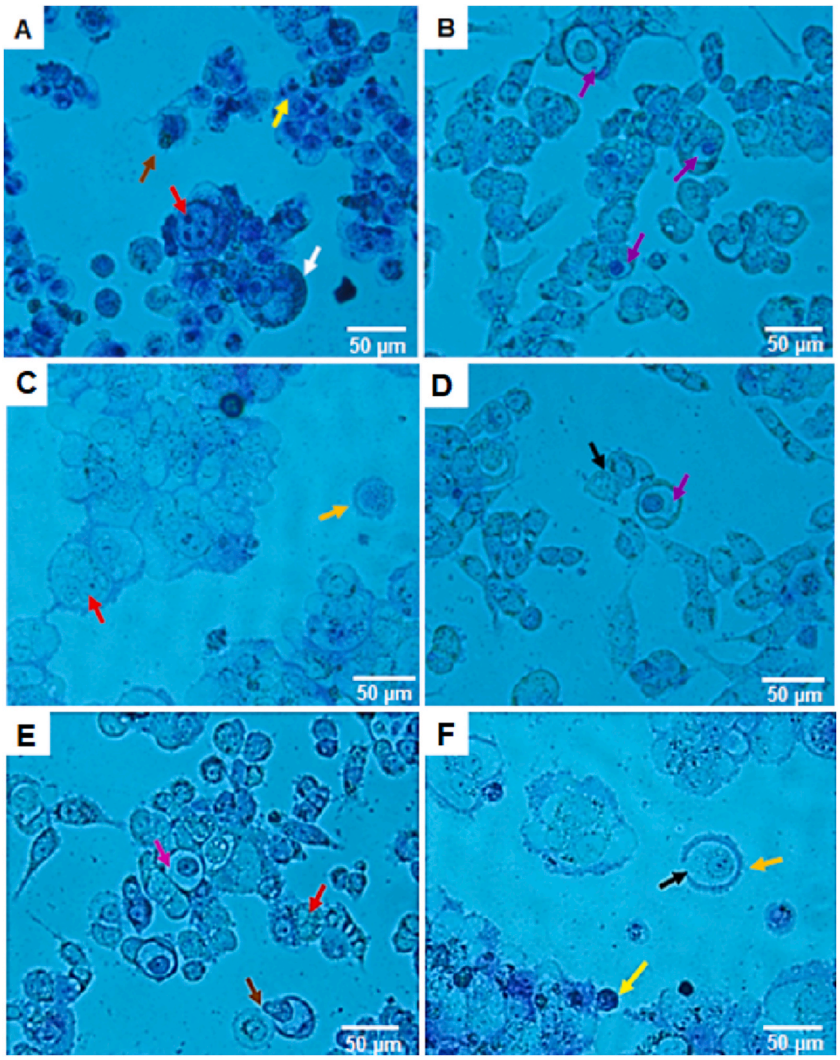

Fig. 2. Apoptosis induced by scutellarein in HT-29 (A, B), SW-480 (C, D), and HCT-116 (E, F) cells. A yellow arrow indicates chromatin condensation, a black arrow ruptured plasma membrane, a brown arrow apoptotic bodies, a white arrow cell swelling, a red arrow nuclear fragmentation, a violet arrow vacuolated cytoplasm, and an orange arrow membrane blebbing. Magnification was 400X; scale bars of 50 μm.

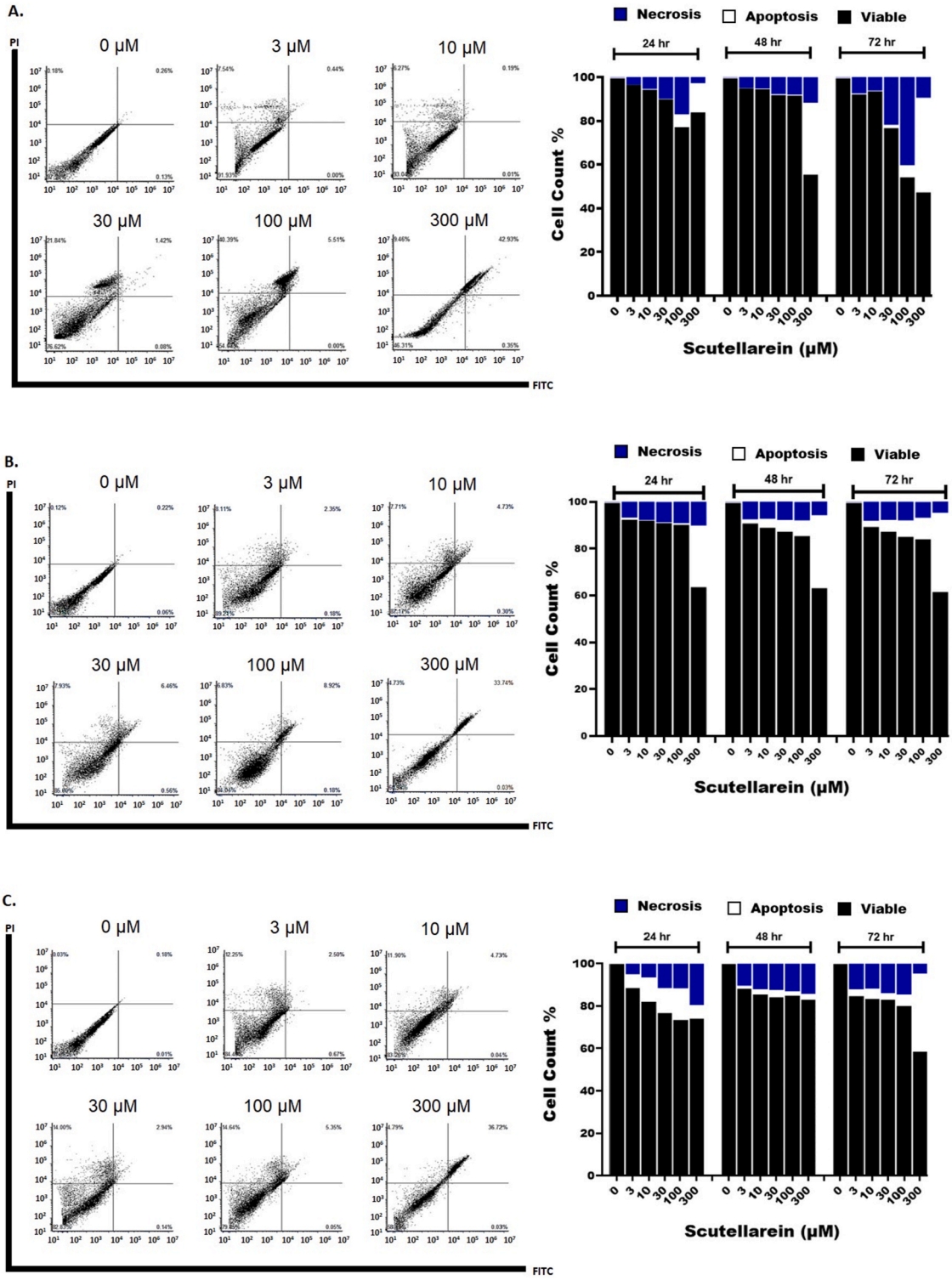

Fig. 3. Representative flow cytometry plots after 72 h (*right panel*). HT-29 (**A**), SW-480 (**B**) and HCT-116 (**C**) cells were treated with the specified concentrations of scutellarein for 24, 48, or 72 h (*left panel*). Flow cytometry plots after incubation of the three cell types for 24 and 48 h are shown in Supplementary Fig. 1 (Fig. S1).

3.4. Wound healing assay

Wound closure test confirmed scutellarein inhibitory effect on migration in the three cell types. Fig. 4 shows that scutellarein inhibited the motility of HT-29, SW-480, and HCT-116 cells and decreased wound closure. The decrease in wound closure (% of the control) was concentration dependent. Wound closure at the highest concentration used (300 μM) ranged between 5 and 10 %.

3.5. Migration and invasion assay

Scutellarein (IC_{50}) reduced the migration ability of the colon cancer cells when compared to the control (Fig. 5A). In addition, Matrigel chamber assay showed that scutellarein reduced the invasion capacity of HT-29 and HCT-116 cells more than SW-480 cells after 72 h of incubation (Fig. 5B).

3.6. Immunofluorescence staining of AQPs 1, 3, and 5

1 HT-29

Fig. 6A showed a marked fluorescence intensity for AQP1 in untreated HT-29 cells when compared to AQP3 or AQP5 (Fig. 6B and **C)**. Scutellarein (IC_{50} = 30.2 μM) decreased the immunopositivity of the 3 AQPs types in HT-29 cells. The mean corrected total cell fluorescence for aquaporins was computed using ImageJ software before and after incubation with scutellarein for 72 h. The fluorescence intensity values for AQP1, AQP3, and AQP5 decreased by 65 %, 35 %, and 60 %, respectively. This decrease was insignificant at $P < 0.05$ for AQP 3 and AQP 5 (Fig. 6A, B, and **C)**.

2 SW-480

The expression patterns of AQPs 1, 3, and 5 are depicted in Fig. 7 in the absence and the presence of scutellarein. Scutellarein, (IC_{50} of 99.2 μM), exhibited a reduction in AQPs 1, 3, and 5 expression in SW-480 cells as compared to the untreated cells (control). The fluorescence intensity values of AQP1, AQP3, and AQP5 exhibited a reduction of 61 %, 56 %, and 77 %, respectively, after an incubation period with scutellarein of 72 h.

3. HCT-116

Upon incubation of HCT-116 cells with scutellarein (IC_{50} of 76.9 μM), AQP1, AQP3, and AQP5 expression was reduced by 66 %, 39 % and 70 % when compared with controls. Although quantification of fluorescence was observed for the 3 AQP types, this reduction was not of a statistical significance at $P < 0.05$ (Fig. 8).

3.7. Reverse transcription-quantitative polymerase chain reaction (RT–qPCR)

3.7.1. PTEN and PI3K gene expression

Treatment of HT-29 cells for 24 h using various concentrations of scutellarein showed an increase in *PTEN* gene expression (2-11-fold). After 48 h of incubation, *PTEN* gene expression was increased at 3, 10 and 30 μM, and markedly upregulated (14-16-fold) in the

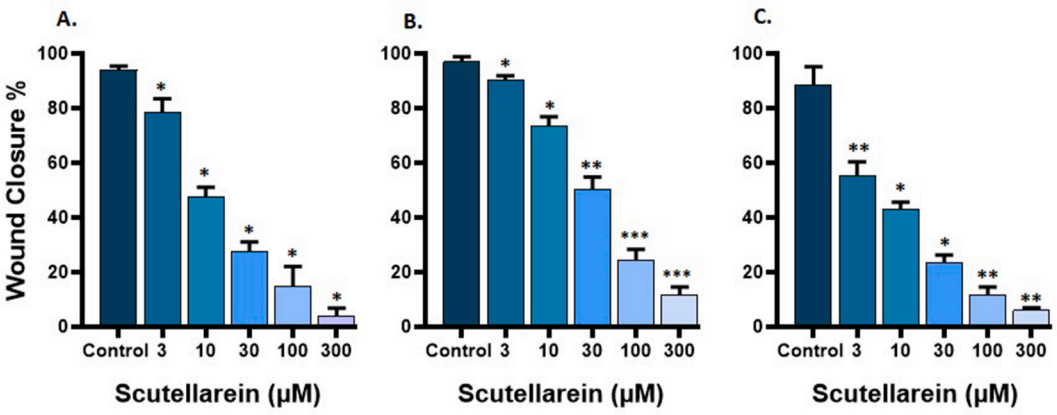

Fig. 4. The inhibitory effect of scutellarein on the wound healing process in (A) HT-29, (B) SW-480, and (C) HC-T116 cell lines. The analysis involved subjecting the assay to various concentrations of scutellarein (0 μM, 3 μM, 10 μM, 30 μM, 100 μM, and 300 μM) for a duration of 72 h. The data obtained from both the control group and the treated groups were subjected to a one-way ANOVA, followed by Dunnett's multiple comparisons test. *$p < 0.05$, **$p < 0.002$ and ***$p < 0.0006$.

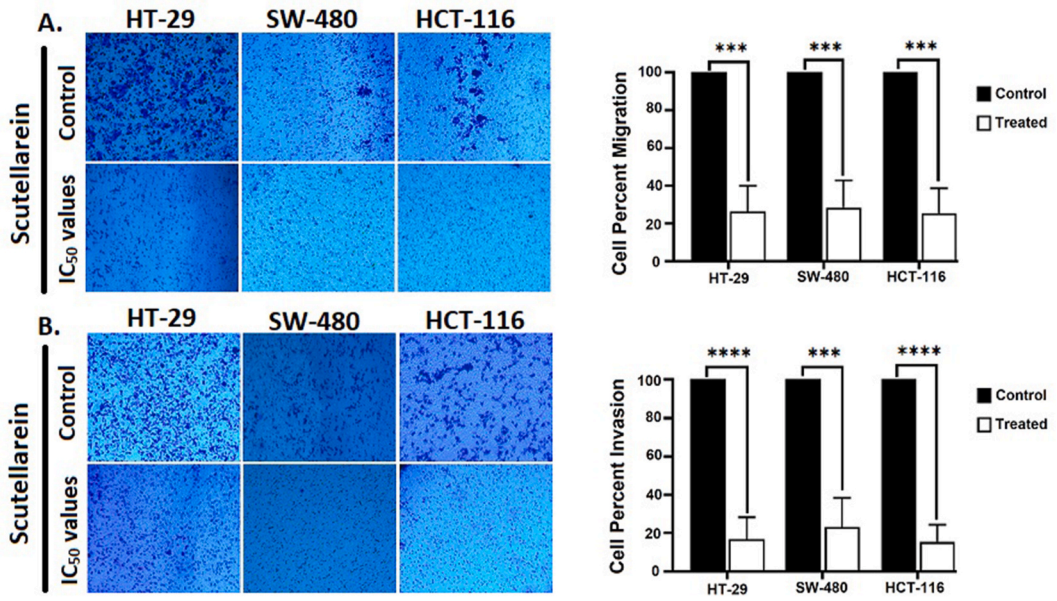

Fig. 5. Effect of scutellarein on HT-29, SW-480, and HCT-116 cell migration (A) and invasion (B) after 72 h of incubation. Transwell chamber assays were used to measure migration, while Matrigel chamber assays were used to measure invasion. For the control and treated groups, two-way ANOVA analysis was done, then Sidak's multiple comparisons test. Magnification was a 40X. ***P< 0.003 and ****P< 0.0001.

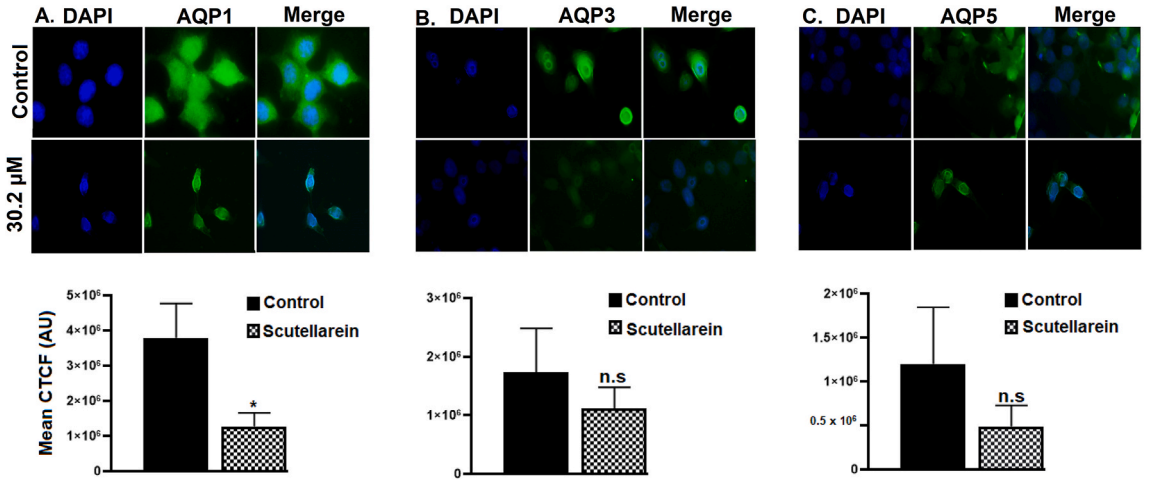

Fig. 6. Scutellarein reduced AQP 1, 3, and 5 staining in HT-29 cells. Immunofluorescence images and quantification of AQP1 (A), AQP3 (B), and AQP5 (C) were obtained before (control) or 72-h incubation with scutellarein IC_{50} (30.2 μM). ImageJ was used to determine the mean adjusted total cell fluorescence for AQP1, AQP3, and AQP5 (http://rsb.info.nih.gov/ij/(NIH), accessed December 23, 2022). Green fluorescence and blue nuclei indicate AQP-positive staining. Analyses used paired t tests. Magnification was 63X with 10 μm scale bars. *P < 0.05; n.s., non-significant (P = 0.15 for AQP3 and P = 0.17 for AQP5).

presence of 100 and 300 μM. After 72 h of treatment, RT−qPCR analysis showed that expression of *PTEN* gene was significantly increased at 3, 10, 30, 100 and 300 μM (9-32-fold) (Fig. 9A).

Fig. 9B shows that *PTEN* gene expression in SW-480 cells was slightly increased in the presence of scutellarein at all tested concentrations after 24 h of incubation (≤2-fold). SW-480 cells treated with 100 and 300 μM scutellarein for 48 h modestly showed increased *PTEN* expression (2-4-fold). A more significant upregulation of gene expression was observed after 72 h. Cells treated with 3 and 10 μM demonstrated a significant increase in gene expression of approximately ≤ 4-fold whereas those treated with 30, 100 and 300 μM showed 6-12-fold increase. Likewise, incubation of HCT-116 cells for 24, 48, and 72 h with scutellarein showed a gradual increase in *PTEN* gene expression (1-3-, 2-4- and 2-7-fold, respectively)., *PTEN* expression was more prominent at higher concentrations (Fig. 9C).

PI3K gene expression was variably expressed when cell lines were incubated with scutellarein. After 24 h of exposure, the gene

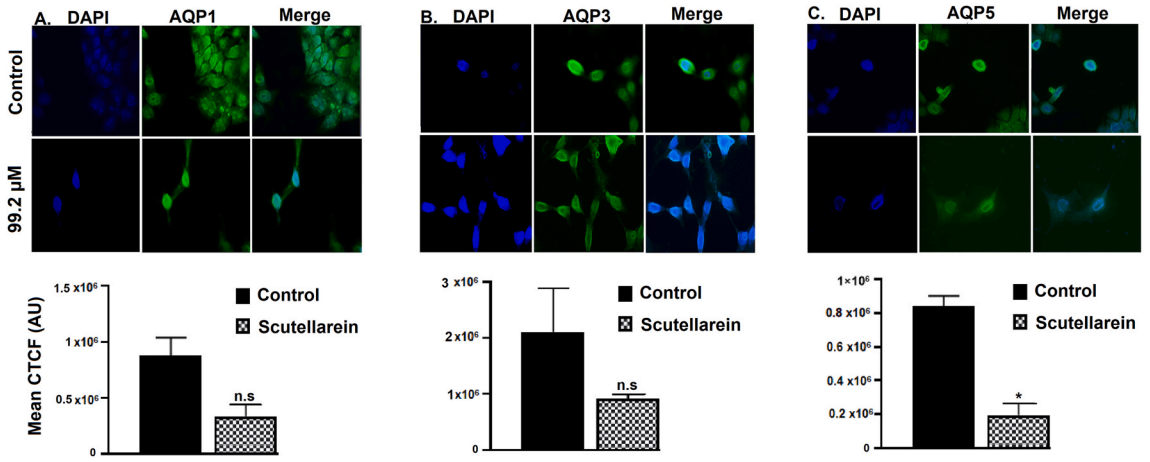

Fig. 7. Scutellarein reduced SW-480 cell AQP 1, 3, and 5 staining intensity. Immunofluorescence images and quantification of AQP1 (A), AQP3 (B), and AQP5 (C) were observed before (control) or 72-h incubation with scutellarein IC_{50} (99.2 μM). ImageJ was used to determine the mean adjusted total cell fluorescence for AQP1, AQP3, and AQP5 (http://rsb.info.nih.gov/ij/(NIH), accessed December 23, 2022). Green fluorescence and blue nuclei indicate AQP-positive staining. Analyses used paired t tests. Magnification was 63X with 10 μm scale bars. *P value < 0.05; n.s., not significant ($P = 0.0501$ for AQP1 and $P = 0.14$ for AQP3).

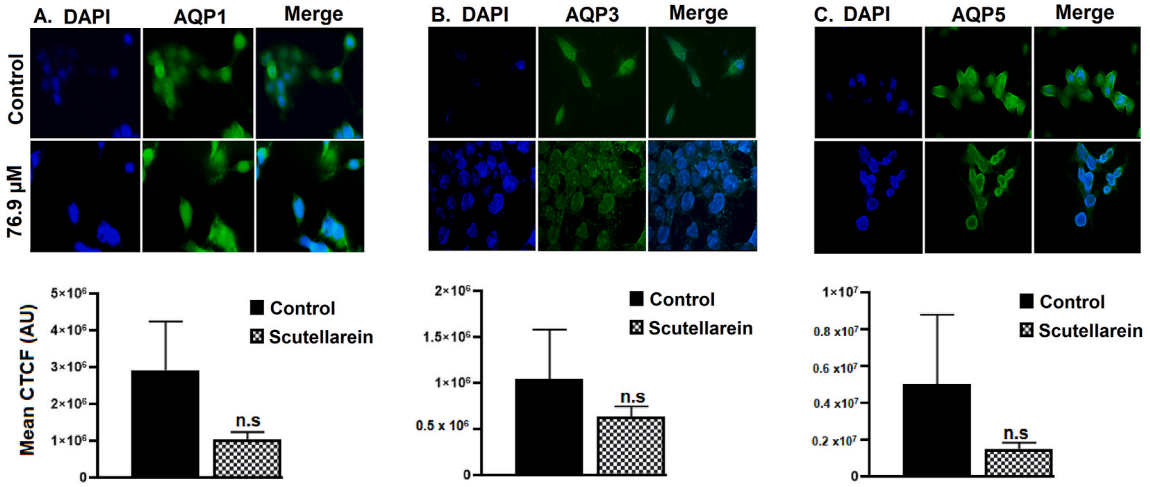

Fig. 8. Scutellarein reduced HCT-116 AQP 1, 3, and 5 staining intensity. Immunofluorescence pictures and quantification of AQP1 (A), AQP3 (B), and AQP5 (C) were taken before (control) and after 72-h incubation with scutellarein (IC_{50}: 76.9 μM). ImageJ was used to determine the mean adjusted total cell fluorescence for AQP1, AQP3, and AQP5. Green fluorescence and blue nuclei indicate AQP-positive staining. Analyses used paired t tests. At 63× magnification and 10 μm scale bars, the P value was not significant ($P = 0.13$ for AQP1 and $P = 0.24$ for AQP3 and AQP5).

expression level in HT-29 cells was insignificantly increased (~2-fold) at 3 and 10 μM, whereas scutellarein significantly reduced the expression at 30, 100 and 300 μM. A reduction in gene expression was also observed after 48 and 72 h at all five concentrations used (Fig. 9D).

In the SW-480 cell line, RT–qPCR analysis showed that expression of *PI3K* gene was downregulated after 24 h of exposure to different concentrations of scutellarein. A similar response was observed after 48 and 72 h. However, *PI3K* gene expression was markedly decreased at 30, 100 and 300 μM after 72 h of exposure (Fig. 9E). When HC-T116 cells were treated with scutellarein, *PI3K* gene expression was upregulated insignificantly at 3, 10 and 30 μM but decreased at 100 and 300 μM after 24 h of incubation. *PI3K* mRNA expression was decreased at all tested concentrations after 48 and 72 h (Fig. 9F).

3.7.2. AQP1, AQP3 and AQP5 gene expression

HT-29 cells exhibited increased *AQP1* gene expression when incubated with 3 or 10 μM of scutellarein for 24 h. However, a slight reduction in gene expression was observed when 30, 100 and 300 μM were used (< 2-fold). After 48 h, gene expression decreased by 5-fold at 300 μM. After 72 h of incubation, the expression of *AQP1* decreased at all concentrations but was remarkably downregulated when cells were treated with 30, 100 and 300 μM (Fig. 10A). SW-480 cells incubated for 24 h with scutellarein exhibited a

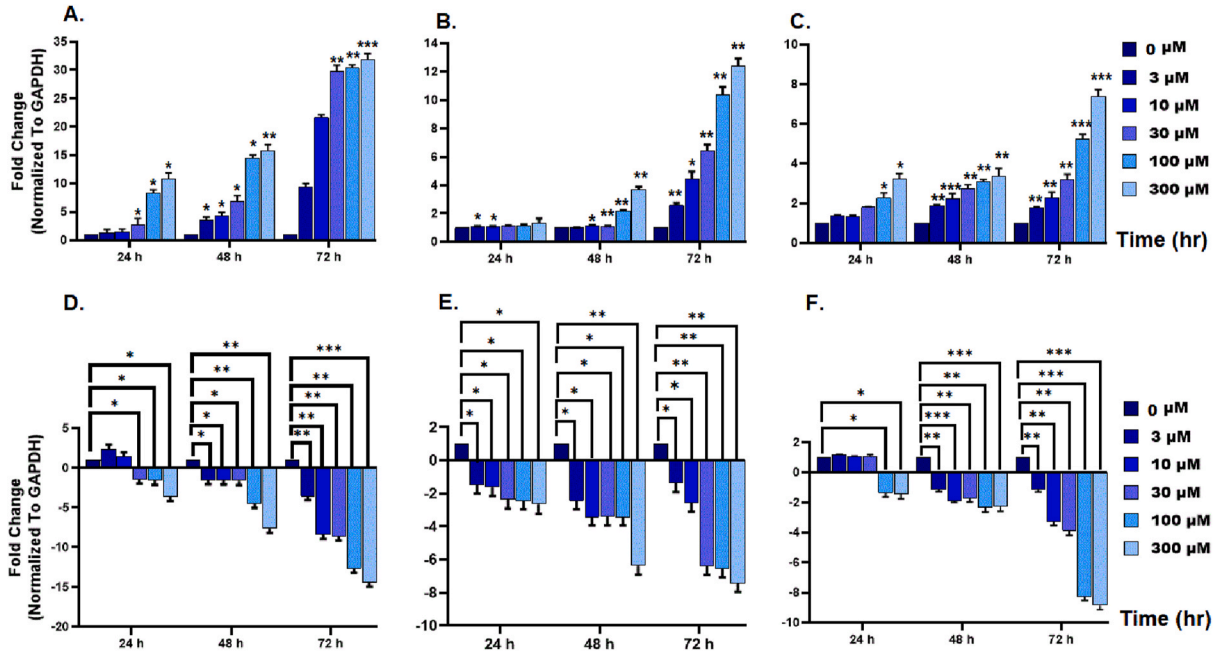

Fig. 9. Scutellarein increased PTEN (*upper panel*) but reduced PI3K (*lower panel*) mRNA expression levels in HT-29 (A, D), SW-480 (B, E) and HCT-116 (C, F) cells. Cells were incubated with the indicated concentrations of scutellarein for 24, 48, and 72 h. Data represent mean ± SD from two independent experiments, assessed using two-way ANOVA for control and treatment groups and Dunnett's multiple comparisons test. *$p < 0.05$, **$p < 0.01$ and ***$p < 0.001$ compared to the control.

downregulation of *AQP1* expression at 3, 10, 30, 100 and 300 µM (< 3-fold). After 48 and 72 h of exposure, the expression of *AQP1* decreased at all tested concentrations but was distinctly downregulated at 300 µM after 72 h (Fig. 10B). Furthermore, HCT-116 cells incubated with scutellarein for 24 h showed a biphasic response starting with a small increase in *AQP1* expression at 3 and 10 µM followed by a decrease at 30, 100 and 300 µM. HC-T116 cells incubated with scutellarein for 48 and 72 h demonstrated persistent downregulation (Fig. 10C).

The *AQP3* gene was differentially expressed in HT-29 cells upon incubation with scutellarein. After 24 h of exposure, the gene expression level was insignificantly increased (< 2-fold) at 3 µM, whereas scutellarein significantly reduced the expression at 10, 30, 100 and 300 µM. A reduction in gene expression was also observed after 48 and 72 h at all five tested concentrations (Fig. 10D). When SW-480 cells were treated with scutellarein for 24 h, *AQP3* expression was insignificantly increased at 3 and 10 µM but decreased at 30, 100 and 300 µM. Cells treated with scutellarein for 48 and 72 h showed a significant reduction in *AQP3* expression at all the tested concentrations (Fig. 10E). Upon incubation of HC-T116 cells with scutellarein, the expression of *AQP3* was dramatically reduced at all concentrations and time points (Fig. 10F).

Fig. 10G shows that *AQP5* gene expression followed a similar trend to that observed with *AQP3* expression in HT-29 cells. Only the lowest concentration (3 µM) of scutellarein was associated with an insignificant upregulation of gene expression after 24 h of exposure. However, a modest downregulation was observed at 10, 30, 100 and 300 µM. After 48 and 72 h, gene expression was downregulated in HT-29 cells at all concentrations, but the effects were more obvious after 72 h especially at 30, 100, and 300 µM (11, 15, and 20-fold, respectively).

Likewise, the same trend of *AQP5* expression in SW-480 cells was noted with all scutellarein concentrations at all time points. Notably, a significant downregulation of gene expression of approximately 11-fold was noted when SW-480 cells were incubated with 300 µM scutellarein after 72 h of incubation (Fig. 10H). Treatment of HC-T116 cells for 24 and 48 h with all tested concentrations of scutellarein caused a decrease in *AQP5* expression. The fold decrease in gene expression after 24 and 48 h of incubation at 300 µM was 4- and 9-fold, respectively. After 72 h of incubation, *AQP5* expression was significantly downregulated at all concentrations, but remarkably at 300 µM (29-fold) (Fig. 10I).

3.7.3. Western blot

Fig. 11A shows that PTEN protein expression was increased in HT-29 cells when incubated with scutellarein for 72 h. Moreover, the data showed that scutellarein slightly decreased the total level of AKT but increased p-AKT at 100 µM. The expression of total mTOR and p-mTOR decreased at all tested concentrations in this cell line.

SW-480 cells incubated for 72 h with scutellarein showed a concentration-dependent increase in *PTEN* gene expression. 10 µM of scutellarein did not produce an effect on the total level of AKT, but higher concentrations significantly reduced AKT protein expression. Phosphorylated AKT (p-AKT) was slightly reduced at all concentrations but significantly reduced at 30 and 100 µM. The relative expression levels of total mTOR and its phosphorylated form (p-mTOR) were reduced when the cells were treated with scutellarein

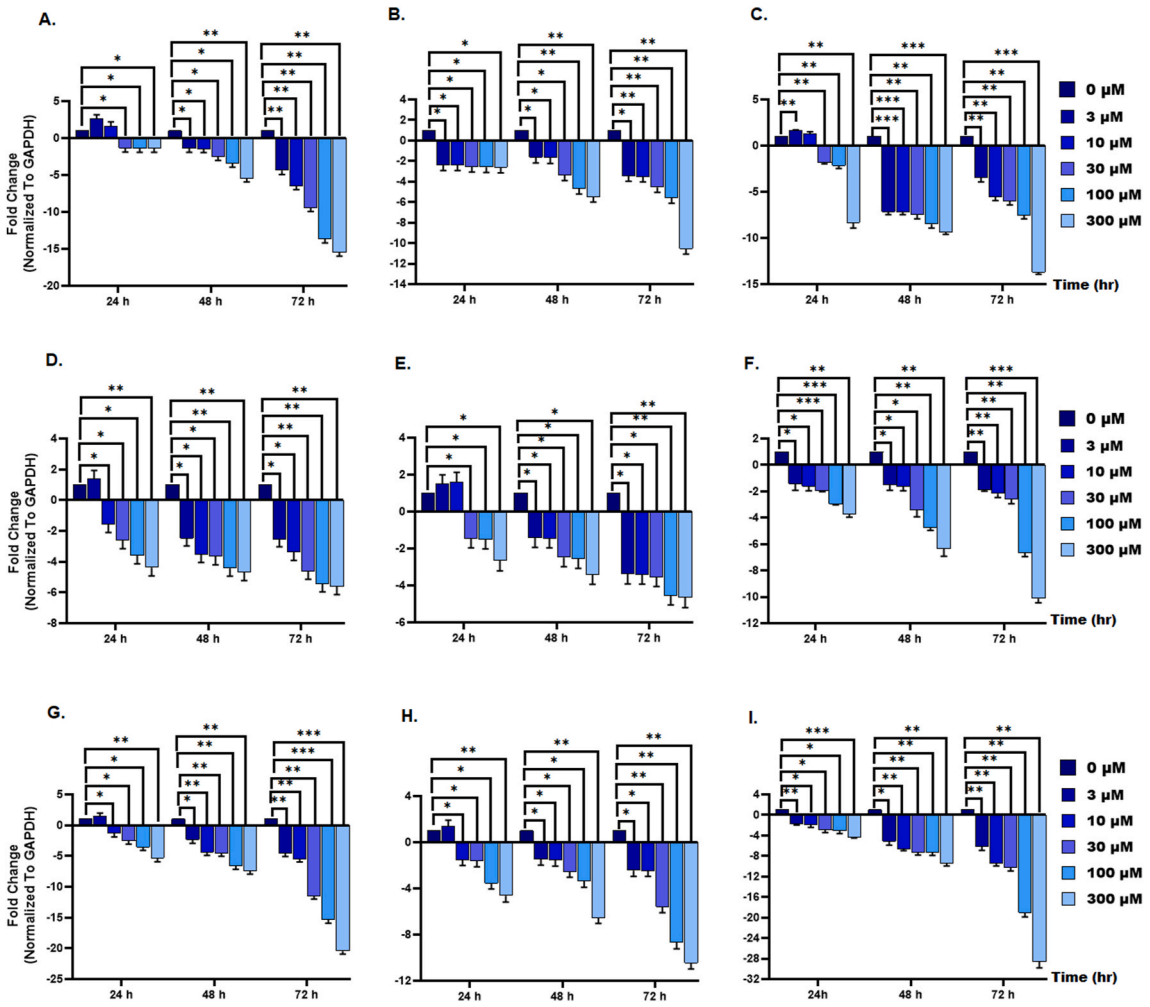

Fig. 10. Scutellarein reduced the mRNA expression levels of AQP1, AQP3, and AQP5 in HT-29 (A, D, G), SW-480 (B, E, H) and HCT-116 (C, F, I) cells. Data represent mean ± SD from two independent experiments, assessed using two-way ANOVA for control and treatment groups and Dunnett's multiple comparisons test. *P < 0.05, **P < 0.01, and ***P< 0.001 when compared to the untreated control.

(Fig. 11B).

Likewise, Western blot analysis showed that PTEN expression increased with increasing concentrations of scutellarein in HC-T116 cells. AKT was slightly reduced and p-AKT was slightly increased, whereas the expressions of total mTOR protein and p-mTOR were reduced (Fig. 11C). Original blots for the proteins from the 3 cell lines are provided as supplementary material (Fig. S2; *Original Western Blots Scutellarein)*.

4. Discussion

Scutellarein (4,5,6,7-tetrahydroxyflavone) is a flavone that possesses anti-inflammatory and antioxidant properties [12], and many studies have shown that scutellarein inhibited viability of lung cancer cells in human, fibrosarcoma cells [13], as well as it showed antitumor activity in human colon cancer [17,39,40]. In fact, scutellarein anticancer activity has been documented against many cancer cells, like hepatic, lung, breast, colon, tongue, ovarian and connective tissue cancers [17]. For example, although there are no effective therapeutic methods available against fibrosarcoma, a type of cancer that affects connective tissue and is classified as aggressive and highly metastatic [41], scutellarein exhibited significant activity against this type of malignancy. Additionally, Shi et al. [13] showed that the rate of proliferation and tumor weight of fibrosarcoma cells (HT1080) were reduced through apoptosis induction after incubation with scutellarein, and that scutellarein inhibited metastasis, invasion, and metalloproteinase activity.

In addition, scutellarein and some natural compounds, such as chrysin, baicalein, sinensetin, and genkwanin, have been found to inhibit the proliferation and decrease the spread of breast cancer cells (MDA-MB-468) before and after the addition of the activation enzymes CYP1A1, CYP1B1 and CYP1A2 since they convert these enzymes into an active form [42]. Moreover, a high concentration of scutellarein (10 µM) suppressed proliferation and activated cell apoptosis by inducing the mitochondrial signaling pathway in oral

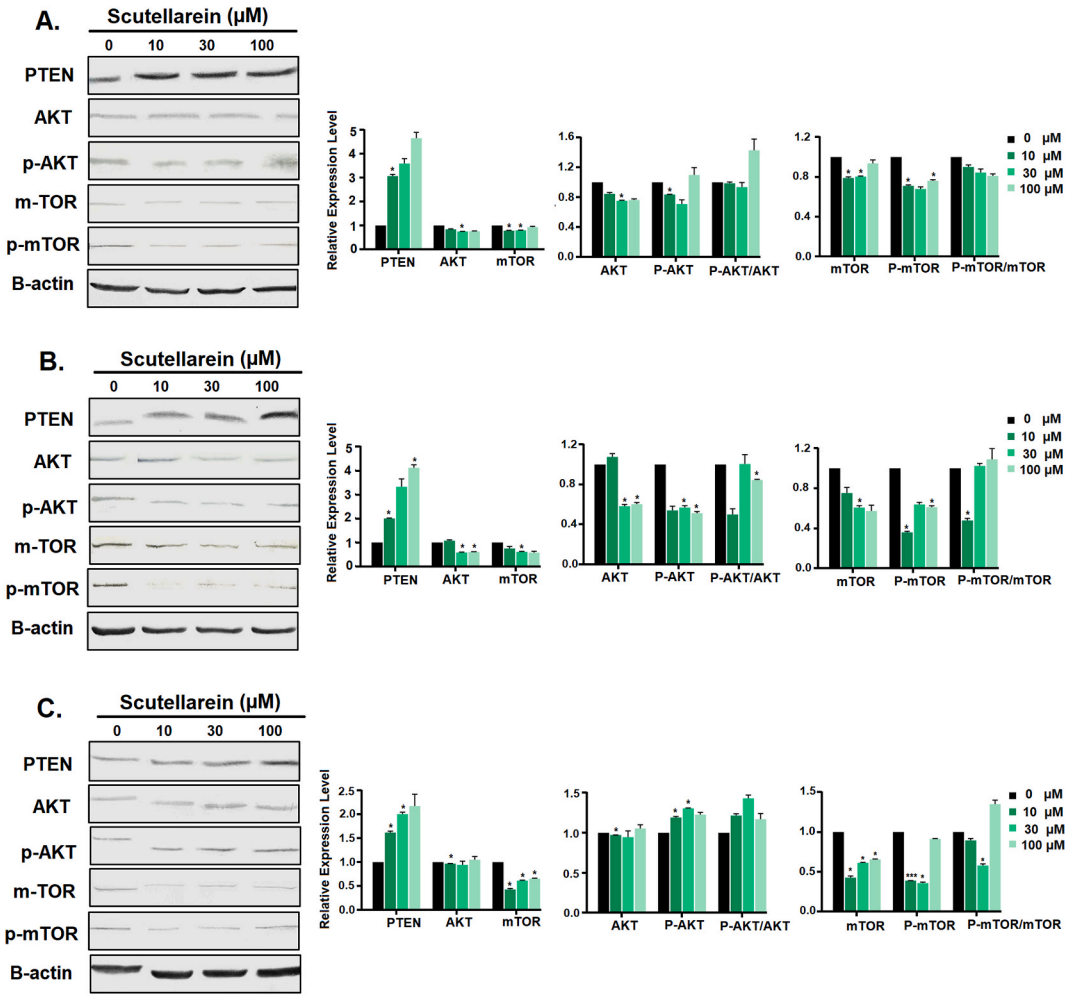

Fig. 11. Western blot demonstrating scutellarein effect on CRC cell line PTEN, AKT, p-AKT, mTOR, and p-mTOR protein expression. (**A**) HT-29, (**B**) SW-480, (**C**) HCT-116. Cells were incubated with scutellarein (0, 10, 30, 100 μM) for 24, 48, and 72 h. Data represent mean ± SD from two independent experiments, assessed using two-way ANOVA for control and treatment groups and Dunnett's multiple comparisons test. *P < 0.05 and ***P< 0.001 when compared to the untreated control. Original blots for the proteins from the 3 cell lines are provided as supplementary material (Fig. S2; *Original Western Blots Scutellarein*).

squamous cell carcinoma [43].

The current study demonstrated that scutellarein had notable anti-CRC activity. MTT assays demonstrated that scutellarein exerted antiproliferative activity on CRC cells. The half maximal inhibitory concentrations of scutellarein against HT-29, SW-480 and HCT-116 cells were 30.2, 99.2, and 76.9 μM, respectively. In our experiment, the IC_{50} values for HT-29 and SW-480 cells were lower than the values reported by Wang et al. [44] (0.099 mM and 0.173 mM, respectively). Recently, Li and coworkers [18] showed that scutellarein inhibited the SW-480 cell line, and the IC_{50} was 39.6 μM, which was lower than what we found in the current study.

Consistent with the MTT data in the present study, flow cytometry analysis revealed that scutellarein caused concentration- and time-dependent reduction in viability of cells and an increased apoptotic and necrotic cell counts. Cell counts showed that HT-29 cells displayed higher sensitivity to scutellarein than SW-480 and HCT-116 cells after 72 h of incubation (apoptosis of 43.3 % of the cells for HT-29 vs. 33.8 % and 36.8 % for the other 2 cell lines, respectively). This is consistent with the MTT data, where the IC_{50} values were 30.2, 99.2, and 76.9 μM.

The above data are partly consistent with those of Guo et al. [17] that showed that scutellarein significantly increased HCT-116 cell apoptosis. These authors found that Hoechst 33258 stain and the fragment DNA assay displayed small nuclei with bright blue staining and a DNA ladder, which indicated that the cells were going through the apoptotic process. Other studies [18] reported scutellarein's apoptotic effect on SW-480 cells and showed that 80 μM increased apoptosis up to 15 % after 24 h. However, we obtained a maximum apoptosis with scutellarein in this cell type of approximately 26.3 % after 24 h with 300 μM.

The current study also demonstrated the impact of scutellarein on colon cancer cell line morphology. Toluidine blue stain was used to demonstrate the apoptotic features of the cells after 72 h of incubation. As demonstrated in Fig. 2, the morphological criteria of

apoptosis in cell lines, including condensation of chromatin, cell swelling, nuclear fragmentation, apoptotic bodies and vacuolated cytoplasm, were observed after 72 h.

Experiments like wound healing, migration or invasion were used to demonstrate the effect of scutellarein on migration capability of the three cell lines. Wound closure data showed that HT-29 and SW-480 cells were less sensitive than HCT-116 cells after 72 h (Fig. 4). Other workers studied the antimigratory impact of scutellarein on HT-29 cells using a transwell assay and found that 80 μg/mL decreased cell migration ability after 24 h [14]. This is consistent with our observations, although the concentration used by these authors was approximately 10x higher than the IC_{50} values that we used, and our incubation time was 72 h compared to the time they used.

Apoptosis is the outcome of cell cycle arrest. Flavones induce apoptosis through several pathways. For example, apigenin induced cell apoptosis in rat embryonic liver (BNLCL-2) cells by upregulating the tumor necrosis factor receptor (TNF-R) and TNF-related apoptosis-inducing ligand factor (TRAIL-R) pathways and downregulating the Bcl2-mediated caspase-dependent pathway [45], whereas chrysin induced apoptosis of HCT-116 cells through the TRAIL-mediated pathway that promoted caspase extrinsic death receptors [46]. CRCs display distinct molecular signatures, and the identification of different molecular pathways is important for prognosis and therapy [47]. Alterations in the PI3K/AKT pathway, such as PI3K mutations, AKT amplification, PTEN loss of function, and mTOR hyperactivation, are common in CRC [48,49]. Growth factors released into the extracellular environment trigger intracellular pathways via tyrosine kinase receptors (RTKs) or G-protein-coupled receptors (GPCRs) on cell membrane. The epithelial growth factor receptor (EGFR) is an RTK that activates PI3K-AKT pathways [50]. When RTKs is stimulated by epithelial growth factors (EGF), PI-3-kinase (PI3K) is recruited to the plasma membrane, leading to stimulation of the enzymatic activity of PI3K. The latter converts PI 4,5-bisphosphate (PIP2) to PI 3,4,5-triphosphate (PIP3), providing docking sites for signaling proteins, including phosphoinositide-dependent kinase (PDK) and AKT. Following activation, AKT activates the downstream mammalian target of rapamycin (mTOR), that regulates proliferation, survival as well as metabolism [49]. The PI3K pathway is regulated negatively by the tumor suppressor phosphatase and tensin (PTEN), which, by counteracting PI3K pathway, reduces PIP3 levels by converting it back to PIP2 because PTEN has a phosphatase activity [51].

Although the anticancer activities of scutellarein have been widely demonstrated, the exact molecular pathway remains unclear. Therefore, although scutellarein inhibits colon cancer proliferation, migration, and invasion [40,52], there are several signaling pathways which seem to be involved in explaining the potential role of scutellarein as an antitumor agent. Various signaling pathways-associated genes have been found to be dysregulated either due to mutations or to function alteration of their products in CRC. Genes like *EGFR*, *PIK3CA*, and *PTEN,* among others were identified to be controlling proliferation, invasion, progression, or suppression of apoptosis in CRC cells [52].

To elucidate the possible mechanism of action of scutellarein, we focused on PI3K/AKT and AQP-mediated activities. RT-qPCR in addition to immunoblotting were used to determine whether scutellarein influenced PTEN and PI3K expression. The results of RT-qPCR showed that expression of PTEN was increased significantly in all tested cell types by scutellarein in a concentration-dependent manner (maximally approximately 8-, 13-, and 33-fold for HT-29, SW-480, and HCT-116 cell lines, respectively). Additionally, the PI3K gene expression was downregulated by 7-fold in SW-480 cells, 9-fold in HC-T116 cells and 15-fold in HT-29 cells after incubation for 72 h with scutellarein at the highest concentration used (Fig. 9D, E, F). These changes induced by scutellarein on PTEN and PI3K expression are consistent with changes at the level of the proteins since PTEN expression was increased (2-5-fold) and AKT, mTOR and p-mTOR were decreased at all concentrations in the 3 cell types (Fig. 11). To our knowledge, this is the only work that investigated the modulatory effect of scutellarein on the *PI3K/PTEN/AKT* pathway in the 3 tested cell lines. This demonstrated that scutellarein caused cell arrest concomitant with upregulation of PTEN and downregulation of PI3K, AKT and mTOR and their downstream targets: p-AKT and p-mTOR proteins.

On the other hand, the expression of AQPs and CRC carcinogenesis have been positively correlated in several studies [3,4]. In consistence with these studies, we showed a pronounced expression of AQP1, AQP3, and AQP5 in the three CRC cell lines using immunofluorescence and RT-qPCR tests. Moreover, we demonstrated a decrease in the immunofluorescence (Figs. 6–8) and in the 3 AQP types expression after incubation of cell lines with scutellarein (Fig. 10).

To understand how AQPs are involved in the anticancer effect, Li et al. [22] provided evidence that hEGF can upregulate AQP3 protein expression as well as migration of colorectal carcinoma cell line HCT-116 in a manner that depends on dose and time. They also showed that CuSO4, an AQP3 inhibitor, impeded the accelerated migration of HCT-116 cells. Similarly, the inhibitor LY294002 of PI3K/AKT inhibited the overexpression of AQP3 induced by hEGF while U0126, an inhibitor of ERK pathway, had no significant effect on hEGF-induced AQP3 upregulation [22]. Zhang et al. [53] showed an increased proliferation and migration in cancer cells with high expression of AQP5, and this AQP5 overexpression caused enhanced activation of EGFR in lung cancer in a positive feedback manner, whereas deletion of AQP5 in a knockdown mouse lung caused lower activation of the EGFR/ERK/MAPK pathway. Others found that human squamous cell carcinoma (A431) EGF-induced growth and migration were reduced in AQP3 knockdown cells when compared to their controls. Therefore, these observations suggested that AQP3 is needed for EGF-EGFR cell signaling in skin cancer cells [54]. Ikarashi et al. [55] treated epidermal keratinocyte HaCaT cells with erlotinib, an anticancer epidermal growth factor receptor tyrosine kinase inhibitor (EGFR-TKI). This treatment revealed that in the erlotinib-treated group only the expression of AQP3 at the mRNA and protein levels was significantly decreased. Erlotinib treatment also significantly suppressed phospho-EGFR and phospho-(ERK) expression. Consistent with these findings that signify the role of AQPs in tumor growth and migration, the current study showed that scutellarein downregulated AQP 1, 3, and 5 expressions in these cells, suggesting a likely role for scutellarein in inhibiting the three cell lines metastasis. To our knowledge, this report is the first to examine scutellarein effect on AQPs expression in these 3 colon cancer cell lines and their impact in the underlying molecular pathways that attenuate cell proliferation.

The current study has provided confirmation of the potential of scutellarein in disrupting the PI3K/AKT/mTOR pathway by

upregulating the tumor suppressor PTEN. PTEN functions as an antagonist to PI3K, leading to the subsequent activation of downstream AKT and mTOR at both the RNA and translational levels. Additionally, this investigation provided evidence of scutellarein's anticancer efficacy by targeting the PTEN/PI3K/AKT/mTOR pathway and downregulating AQP1, AQP3, and AQP5 expression. According to previous research, it has been proposed that growth factors, such as hEGF, can increase the expression of AQPs. This upregulation of AQPs expression is believed to contribute to the promotion of malignancies by facilitating cell migration [22]. Specifically, it has been shown that hEGF can induce the extension of lamellipodia, which are the leading edges of migratory cells, and accelerate the overall pace of cell movement. The finding that scutellarein has the ability to increase the expression of PTEN while decreasing the expression of PI3K, AKT, and mTOR, as well as AQPs 1, 3, and 5, simultaneously provides evidence for the diverse impact of scutellarein. This finding also offers insights into the potential interplay of AQPs and other molecular pathways, specifically the PI3K/AKT signaling pathway and its downstream targets, mTOR and p-mTOR as illustrated in Fig. 12.

Limitation to the study: This investigation was carried out *in vitro*. While *in vitro* experiments give useful insights, they do not fully duplicate the intricate interactions found in actual organisms. Therefore, the findings may not be immediately transferable to *in vivo* or translatable to the clinical setting. Furthermore, the study used a small number of cancer cell lines, which may not accurately represent the diversity of cancer types and subtypes which differ in the origin from which they were derived [56], in their shape (epithelioid vs. stellate [57]) and their ability of migration, invasion, and aggressiveness as well as their differential expression of the different types of aquaporins [58,59]. Different malignancies may demonstrate a variety of AQP-related behaviors and responses. Another constraint of this work is that AQP expression levels were evaluated by quantitative PCR. Although these methods are valuable, they may not provide an accurate picture of the protein function and localization in the cell. Moreover, the study examined the influence of scutellarein on the PI3K/AKT/PTEN pathway; however, there are several pathways that may be affected, so knowing the crosstalk among these pathways is crucial for developing targeted therapeutics. Finally, efforts should be made to minimize the off-target effects of the molecule by structural manipulation in order to enhance its bioavailability and the other pharmacokinetics parameters since it has been found that scutellarein inhibits uridine 5′-diphosphate glucuronide transferases as well as cytochrome P450 enzyme, thus posing some side effects [60].

5. Conclusion

The present work confirms previous reports that scutellarein could therapeutically target colon tumor proliferation and metastasis. In addition, this work provides evidence that scutellarein plays a significant role as a potent activator of PTEN, thereby inhibiting PI3K signaling pathways in CRC cells. It also demonstrates that scutellarein downregulates aquaporins, the molecules implicated in

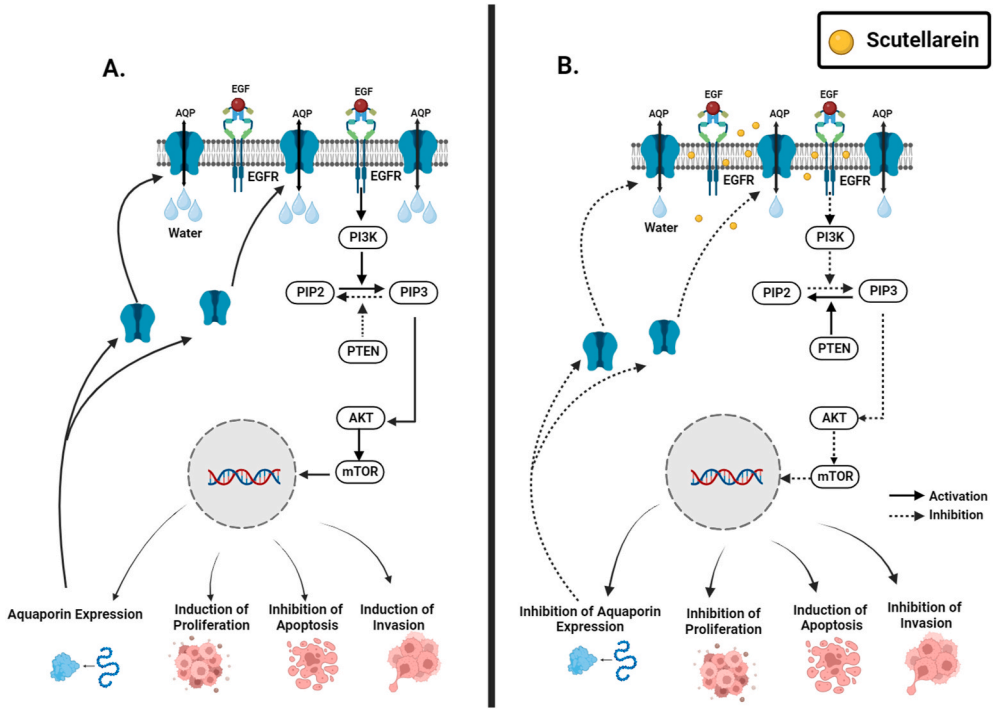

Fig. 12. Hypothetical mechanism of action of scutellarein. (A) In the canonical form, epidermal growth factor receptor (EGFR), located in lipid rafts, dimerizes in the presence of epidermal growth factor (EGF) and initiates a signaling cascade that allosterically activates PI3K, making the pathway active to produce AKT and downstream targets, thus stimulating the expression of AQPs, which facilitate cell migration. (**B**) In the presence of scutellarein, the PI3K/AKT/mTOR pathway is disrupted to upregulate tumor suppressor phosphatase and tensin (PTEN). Upregulation of PTEN results in downregulation of AQP expression and inhibition of cell proliferation, invasion, and metastasis.

enhancing the metastasis of cancer cells. The findings provide new insight into the molecular mechanism of scutellarein's antineoplastic role in CRC cells, as well as its role in survival, and confirm the pleiotropic effects of scutellarein.

Funding

This work was funded by The University of Jordan; Grant # 19/2020/1204.

CRediT authorship contribution statement

Noor Tarawneh: Writing – original draft, Visualization, Software, Resources, Methodology, Investigation, Formal analysis, Data curation. **Lama Hamadneh:** Writing – review & editing, Methodology, Investigation, Formal analysis, Data curation. **Walhan Alshaer:** Writing – review & editing, Validation, Software, Methodology, Formal analysis, Data curation. **Abdel Qader Al Bawab:** Writing – review & editing, Software, Resources, Methodology, Formal analysis, Data curation. **Yasser Bustanji:** Writing – review & editing, Supervision, Project administration, Methodology, Investigation, Conceptualization. **Shtaywy Abdalla:** Writing – review & editing, Validation, Supervision, Project administration, Funding acquisition, Conceptualization.

Data and code availability statement

Data included in the article/supplementary material is referenced in the article.

Declaration of competing interest

The authors declare that they have no known competing financial interests or personal relationships that could have appeared to influence the work reported in this paper.

Appendix A. Supplementary data

Supplementary data to this article can be found online at https://doi.org/10.1016/j.heliyon.2024.e39402.

References

[1] T. Sawicki, M. Ruszkowska, A. Danielewicz, E. Niedźwiedzka, T. Arłukowicz, E. Przybyłowicz, A review of colorectal cancer in terms of epidemiology, risk factors, development, symptoms and diagnosis, Cancers (Basel) 13 (9) (2021) 2025–2048, https://doi.org/10.3390/cancers13092025.
[2] P.S. Steeg, Targeting metastasis, Nat. Rev. Cancer 16 (4) (2016) 201–218, https://doi.org/10.1038/nrc.2016.25.
[3] B. Kang, J. Kim, S. Lee, Y. Chae, J. Jeong, G. Yoon, et al., Expression of aquaporin-1, aquaporin-3, and aquaporin-5 correlates with nodal metastasis in colon cancer, Oncology 88 (2015) 369–376, https://doi.org/10.1159/000369073.
[4] W. Wang, Q. Li, T. Yang, D. Li, F. Ding, H. Sun, et al., Anticancer effect of aquaporin 5 silencing in colorectal cancer cells in association with inhibition of Wnt/β-catenin pathway, Cytotechnology 70 (2018) 615–624, 10.1007%2Fs10616-017-0147-7.
[5] S. Moon, D. Moon, K. Kang, Aquaporins in cancer biology, Front. Oncol. 12 (2022) 782829–782845, https://doi.org/10.3389/fonc.2022.782829.
[6] A. Allegra, N. Cicero, G. Mirabile, G. Cancemi, A. Tonacci, C. Musolino, Critical role of aquaporins in cancer: focus on hematological malignancies, Cancers 14 (2022) 4182, https://doi.org/10.3390/cancers14174182.
[7] E. Migliati, N. Meurice, P. DuBois, S. Fang, S. Somasekharan, E. Beckett, Inhibition of aquaporin-1 and aquaporin-4 water permeability by a derivative of the loop diuretic bumetanide acting at an internal pore-occluding binding site, Mol. Pharmacol. 76 (1) (2009) 105–112, https://doi.org/10.1124/mol.108.053744.
[8] S. Verkman, J. Smith, W. Phuan, L. Tradtrantip, O. Anderson, The aquaporin-4 water channel as a potential drug target in neurological disorders, Exp Opin Therap Targ 21 (12) (2017) 1161–1170, https://doi.org/10.1080/14728222.2017.1398236.
[9] J. Escalante, R.M. McQuade, V. Stojanovska, N. Kulmira, Impact of chemotherapy on gastrointestinal functions and the enteric nervous system, Maturitas 105 (2017) 23–29.
[10] Y.Z. Cai, M. Sun, J. Xing, Q. Luo, H. Corke, Structure-radical scavenging activity relationships of phenolic compounds from traditional Chinese medicinal plants, Life Sci. 74 (2005) 2157–2184.
[11] F. Memari, F. Mirzavi, M. Jalili-Nik, A.R. Afshari, A. Ghorbani, M. Soukhtanloo, Tumor-inhibitory effects of zerumbone against HT-29 human colorectal cancer cells, Intl J Toxicol 41 (5) (2022) 402–411, https://doi.org/10.1177/10915818221104417.
[12] W. Eric, C. Choo, S. Carine, S. Lim, W. Lim, Z. Loong, et al., Role of scutellarin in human cancer- A review, J Appl Pharma Sci 9 (1) (2019) 142–146, https://doi.org/10.7324/JAPS.2019.90119.
[13] X. Shi, G. Chen, X. Liu, Y. Qiu, S. Yang, Y. Zhang, et al., Scutellarein inhibits cancer cell metastasis in vitro and attenuates the development of fibrosarcoma in vivo, Int. J. Mol. Med. 35 (2015) 31–38, https://doi.org/10.3892/ijmm.2014.1997.
[14] Z. Xiaoyue, W. Jiejun, Y. Guanzhen, W. Zhan, J. Xiaodong, L. Ke, et al., Effect and mechanism of scutellarein in suppressing the migration and proliferation of colorectal cancer HT-29 cells, Chin. Clin. Oncol. 20 (3) (2015) 208–210, 10.3389%2Ffonc.2022.956793.
[15] Y. Cheng, C. Hu, J. Yang, C. Lee, S. Kao, Inhibitory effects of scutellarein on proliferation of human lung cancer A549 cells through ERK and NFκB mediated by the EGFR pathway, Chin. J. Physiol. 57 (2014) 182–187, https://doi.org/10.4077/CJP.2014.BAC200.
[16] L. Shi, Y. Wu, L. Lv, L. Feng, Scutellarein selectively targets multiple myeloma cells by increasing mitochondrial superoxide production and activating intrinsic apoptosis pathway, Biomed Pharmacol 109 (2019) 2109–2118, https://doi.org/10.1016/j.biopha.2018.09.024.
[17] F. Guo, F. Yang, H. Zhu, Scutellarein from *Scutellaria barbata* induces apoptosis of human colon cancer HCT116 cells through the ROS-mediated mitochondria-dependent pathway, Nat. Prod. Res. 33 (2019) 2372–2375, https://doi.org/10.1080/14786419.2018.1440230.
[18] Y. Li, J. Wang, S. Zhong, J. Li, W. Du, Scutellarein inhibits the development of colon cancer via CDC4-mediated RAGE ubiquitination, Int. J. Mol. Med. 45 (4) (2020) 1059–1072, https://doi.org/10.3892/ijmm.2020.4496.
[19] X. Lang, C. Zheng, Y. Xingyu, Q. Yan, M. Xu, W. Liu, et al., Scutellarein induces apoptosis and inhibits proliferation, migration, and invasion in ovarian cancer via inhibition of EZH2/FOXO1 signaling, Biochem Mol Toxic 35 (10) (2021) 1–14, https://doi.org/10.1002/jbt.22870.

[20] H.S. Dorward, A. Du, A. Bruhn, J. Wrin, V. Pei, A. Evdokiou, et al., Pharmacological blockade of aquaporin-1 water channel by AqB013 restricts migration and invasiveness of colon cancer cells and prevents endothelial tube formation in vitro, J. Exp. Clin. Cancer Res. 35 (2016) 36–45, 10.1186%2Fs13046-016-0310-6.

[21] L. De Ieso, J. Yool, Mechanisms of aquaporin-facilitated cancer invasion and metastasis, Front. Chem. 6 (2018) 135–155, https://doi.org/10.3389/fchem.2018.00135.

[22] A. Li, D. Lu, Y. Zhang, J. Li, Y. Fang, F. Li, et al., Critical role of aquaporin-3 in epidermal growth factor-induced migration of colorectal carcinoma cells and its clinical significance, Oncol. Rep. 29 (2013) 535–540, https://doi.org/10.3892/or.2012.2144.

[23] N. Tarawneh, L. Hamadneh, B. Abu-Irmaileh, Z. Shraideh, Y. Bustanji, S. Abdalla, Berberine inhibited growth and migration of human colon cancer cell lines by increasing phosphatase and tensin and inhibiting aquaporins 1, 3 and 5 expressions, Molecules 28 (2023) 3823, https://doi.org/10.3390/molecules28093823.

[24] X. Gong, X. Hu, L. Xu, H. Yang, L. Zong, C. Wang, et al., Berberine inhibits proliferation and migration of colorectal cancer cells by downregulation of GRP78, Anti Cancer Drugs 31 (2) (2019) 141–149, https://doi.org/10.1097/cad.0000000000000835.

[25] N. Saleh, H.E. Mahmoud, H. Eltaher, M. Helmy, L.K. El-Khordagui, A. Hussein, Prodigiosin-functionalized probiotic ghosts as a bioinspired combination against colorectal cancer cells, Prob Antim Pro (2022) 1–16, https://doi.org/10.1007/s12602-022-09980-y.

[26] W. Liao, G. Li, Y. You, H. Wan, Q. Wu, C. Wang, et al., Antitumor activity of Notch 1 inhibition in human colorectal carcinoma cells, Oncol. Rep. 39 (3) (2018) 1063–1071, 10.3892%2For.2017.6176.

[27] M. Almeida, R. Alencar Bezerra, C. Nascimento, L. Amorim, Anticancer drug screening: standardization of in vitro wound healing assay, J Brasil Pathol Med Lab 55 (2019) 606–619, https://doi.org/10.5935/1676-2444.20190054.

[28] X. Liu, Q. Ji, N. Ye, H. Sui, L. Zhou, L. Zhu, et al., Berberine inhibits invasion and metastasis of colorectal cancer cells via COX-2/PGE2 mediated JAK2/STAT3 signaling pathway, PLoS One 10 (2015) 1–18, https://doi.org/10.1371/journal.pone.0123478.

[29] Z. Pan, J. Cai, J. Lin, H. Zhou, J. Peng, J. Liang, et al., A novel protein encoded by circFNDC3B inhibits tumor progression and EMT through regulating snail in colon cancer, Mol. Cancer 19 (2020) 71–86, https://doi.org/10.1186/s12943-020-01179-5.

[30] M. Shen, L.Z. Bao, X. Zheng, X.X. Zhao, Z.F. Guo, Obestatin downregulating aquaporin 2 plasma membrane distribution through a short-term regulatory effect, Am. J. Med. Sci. 357 (2019) 247–254, https://doi.org/10.1016/j.amjms.2018.12.010.

[31] C. Bierhals, A. Howard, H. Hirst, Reduction of rapid proliferating tumor cell lines by inhibition of the specific glycine transporter GLYT1, Biomedicines 9 (2021) 1770–1784, https://doi.org/10.3390/biomedicines9121770.

[32] A. Samad, Z. Saiman, A. Majid, A. Karsani, S. Yaacob, Berberine inhibits telomerase activity and induces cell cycle arrest and telomere erosion in colorectal cancer cell line, HCT 116, Molecules 26 (2021) 376–392, https://doi.org/10.3390/molecules26020376.

[33] T.M.K. Motawi, Y. Bustanji, S. El-Maraghy, M.O. Taha, M.A.S. Al-Ghussein, Evaluation of naproxen and cromolyn activities against cancer cells viability, proliferation, apoptosis, p53 and gene expression of survivin and caspase-3, J. Enzym. Inhib. Med. Chem. 29 (2014) 153–161, https://doi.org/10.3109/14756366.2012.762645.

[34] S. Kim, C. Domon-Dell, J. Kang, D.H. Chung, J.N. Freund, B.M. Evers, Downregulation of the tumor suppressor PTEN by the tumor necrosis factor-alpha/nuclear factor-kappaB (NF-kappaB)-inducing kinase/NF-kappaB pathway is linked to a default IkappaB-alpha autoregulatory loop, J. Biol. Chem. 279 (6) (2004) 4285–4291, https://doi.org/10.1074/jbc.m308383200.

[35] H. Shi, J. Pu, L. Zhou, Y. Ning, C. Bai, Silencing long noncoding RNA ROR improves sensitivity of non-small cell lung cancer to cisplatin resistance by inhibiting PI3K/Akt/mTOR signaling pathway, Tumor Biol. 39 (5) (2017) 1–11, https://doi.org/10.1177/1010428317697568.

[36] Y. Fan, M. Ma, X. Feng, T. Song, Q. Wei, R. Lin, Overexpression of aquaporin 2 in renal tubular epithelial cells alleviates pyroptosis, Transl. Androl. Urol. 10 (6) (2021) 2340–2350, 10.21037%2Ftau-21-71.

[37] E. Namkoong, Y.H. Shin, J.S. Bae, S. Choi, Kim N. KimM, et al., Role of sodium bicarbonate cotransporters in intracellular pH regulation and their regulatory mechanisms in human submandibular glands, PLoS One 10 (9) (2015) 1–16, https://doi.org/10.1371/journal.pone.0138368.

[38] A. Čipak Gašparović, L. Milković, C. Rodrigues, M. Mlinarić, G. Soveral, Peroxiporins are induced upon oxidative stress insult and are associated with oxidative stress resistance in colon cancer cell lines, Antioxidants 10 (11) (2021) 1856–1867, 10.3390%2.

[39] L. Xiong, L. Du, L. Xue, Y. Jiang, J. Huang, L. Chen, et al., Anti-colorectal cancer effects of scutellarin revealed by genomic and proteomic analysis, Chin. Med. 15 (2020) 28–43, https://doi.org/10.1186/s13020-020-00307-z.

[40] D. Goh, H. Lee, S. Ong, Inhibitory effects of a chemically standardized extract from Scutellaria barbata in human colon cancer cell lines, LoVo J Agri Food Chem 53 (21) (2005) 8197–8204, https://doi.org/10.1021/jf051506.

[41] D. Augsburger, P. Nelson, T. Kalinski, A. Udelnow, T. Knösel, M. Hofstetter, et al., Current diagnostics and treatment of fibrosarcoma –perspectives for future therapeutic targets and strategies, Oncotarget 8 (61) (2017) 104638–104653, https://doi.org/10.18632/oncotarget.20136.

[42] V. Androutsopoulos, K. Ruparelia, R. Aroo, A. Tsataskis, D. Spandidos, CYP1-mediated antiproliferative activity of dietary flavonoids in MDA-MBA-468 breast cancer cells, Toxicology 264 (2009) 162–170, https://doi.org/10.1016/j.tox.2009.07.023.

[43] G. Jing, J. Zheng, X. Wang, Scutellarein ameliorates tongue cancer cells via mitochondria, Cent. Eur. J. Med. 9 (2014) 193–199, https://doi.org/10.2478/s11536-013-0269-z.

[44] F. Wang, B. Yang, Y. Zhao, X. Liao, C. Gao, R. Jiang, et al., Host-guest inclusion system of scutellarein with 2-hydroxypropyl-beta-cyclodextrin: preparation, characterization, and anticancer activity, J. Biomater. Sci. Polym. Ed. 25 (6) (2014) 594–607, https://doi.org/10.1080/09205063.2014.884875.

[45] A. Khan, H. Dagur, M. Khan, N. Malik, M. Alam, M. Mushtaque, Therapeutic role of flavonoids and flavones in cancer prevention: current trends and future perspectives, Eur J Med Chem Rep 3 (2021) 100010–100026, https://doi.org/10.1016/j.ejmcr.2021.100010.

[46] M. Talebi, M. Talebi, T. Farkhondeh, Emerging cellular and molecular mechanisms underlying anticancer indications of chrysin, Cancer Cell Int. 21 (1) (2021) 214–234, https://doi.org/10.1186/s12935-021-01906-y.

[47] L. Salvatore, M. Calegari, F. Loupakis, M. Fassan, B. Di Stefano, M. Bensi, et al., PTEN in colorectal cancer: shedding light on its role as predictor and target, Cancers (Basel) 11 (11) (2019) 1765–1780, 10.3390%2Fcancers11111765.

[48] H. Zhang, W. Du, X. Guo, L. Wang, J. Cheng, L. Wei, Identification of the AQP8-miR-92a network associated with the aggressive traits of colorectal cancer, Biochem Biophy Res Comm 527 (1) (2020) 218–225, https://doi.org/10.1016/j.bbrc.2020.04.055.

[49] Y. He, M. Sun, G. Zhang, J. Yang, S. Chen, W. Xu, et al., Targeting PI3K/AKT signal transduction for cancer therapy, Signal Transduct. Targeted Ther. 6 (1) (2021) 425–444, https://doi.org/10.1038/s41392-021-00828-5.

[50] F. Molinari, M. Frattini, Functions and regulation of the PTEN gene in colorectal cancer, Front. Oncol. 3 (2014) 326–334, 10.3389%2Ffonc.2013.00326.

[51] A. Hervieu, S. Kermorgant, The Role of PI3K in Met Driven Cancer: A Recap Front Mol Bio, vol. 5, 2018, pp. 86–97, 10.3389%2Ffmolb.2018.00086.

[52] Z. Koveitypour, F. Panahi, M. Vakilian, M. Peymani, F. Seyed, M. Nasr Esfahani, et al., Signaling pathways involved in colorectal cancer progression, CellBio 9 (2019) 97–111, https://doi.org/10.1186/s13578-019-0361-4.

[53] Z. Zhang, Z. Chen, Y. Song, P. Zhang, J. Hu, C. Bai, Expression of aquaporin 5 increases proliferation and metastasis potential of lung cancer, J. Pathol. 221 (2) (2010) 210–220, https://doi.org/10.1002/path.2702.

[54] M. Hara-Chikuma, S. Watanabe, H. Satooka, Involvement of aquaporin-3 in epidermal growth factor receptor signaling via hydrogen peroxide transport in cancer cells, Biochem. Biophys. Res. Commun. 471 (4) (2016) 603–612, https://doi.org/10.1016/j.bbrc.2016.02.010.

[55] N. Ikarashi, M. Kaneko, T. Watanabe, R. Kon, M. Yoshino, T. Yokoyama, et al., Epidermal growth factor receptor tyrosine kinase inhibitor erlotinib induces dry skin via decreased in aquaporin-3 expression, Biomolecules 10 (4) (2022) 545–557, https://doi.org/10.3390/biom10040545.

[56] M.J.A. Van Erk, C.A.M. Krul, E. Caldenhoven, R.H. Stierum, W.H. Peters, R.A. Woutersen, et al., Expression profiling of colon cancer cell lines and colon biopsies: towards a screening system for potential cancer-preventive compounds, Eur. J. Cancer Prev. 14 (2005) 439–457, https://doi.org/10.1097/01.cej.0000174781.51883.21.

[57] N.J. de Both, M. Vermey, W.N. Dinjens, F.T. Bosman, A comparative evaluation of various invasion assays testing colon carcinoma cell lines, Br. J. Cancer 81 (1999) 934–941, https://doi.org/10.1038/sj.bjc.6690790.

[58] J. Ronen, S. Hayat, A. Akalin, Evaluation of colorectal cancer subtypes and cell lines using deep learning, Life Sci. Alliance 2 (2019) e201900517, https://doi.org/10.26508/lsa.201900517.
[59] K.A. Heck, H.T. Lindholm, B. Niederdorfer, E. Tsirvouli, M. Kuiper, Å. Flobak, et al., Characterisation of colorectal cancer cell lines through proteomic profiling of their extracellular vesicles, Proteomes 11 (2023) 3, https://doi.org/10.3390/proteomes11010003.
[60] J. Lai, C. Li, Review on the pharmacological effects and pharmacokinetics of scutellarein, Arch. Pharm. (2024) e2400053, https://doi.org/10.1002/ardp.202400053 wileyonlinelibrary.com/journal/ardp | 1 of 15.